

Article

# Integrated Detection of a Complex Underground Water Supply Pipeline System in an Old Urban Community in China

Shifan Deng <sup>1,2</sup>, Siyu Ma <sup>1,2</sup>, Xiaowen Zhang <sup>1,2</sup> and Shiqiang Zhang <sup>1,2,\*</sup> 

<sup>1</sup> College of Urban and Environmental Science, Northwest University, Xi'an 710127, China; dengshifan@stumail.nwu.edu.cn (S.D.); maasiyu@163.com (S.M.); zhangxw@nwu.edu.cn (X.Z.)

<sup>2</sup> Shaanxi Key Laboratory of Earth Surface System and Environmental Carrying Capacity, College of Urban and Environmental Sciences, Northwest University, Xi'an 710127, China

\* Correspondence: zhangsq@nwu.edu.cn

Received: 8 January 2020; Accepted: 21 February 2020; Published: 23 February 2020



**Abstract:** An underground water supply pipeline system is an integral part of urban infrastructure. The safety, stability, reliability, and efficiency of this water system are critical for the daily work and livelihood of the people dependent on it. However, with the development of cities in China, the water supply systems in urban communities require constant re-building and improvement, which complicates the system. Considering the defects of obsolete design, lack of information, and irregularity of the constructions over the years, the maintenance of underground pipelines in older communities is onerous and arduous. In this work, the older pipeline system at the Taibai campus of Northwest University, Shaanxi Province, was taken as one typical old urban community and investigated by different measures. Detection was performed from the available concentrated water supply wells to surrounding areas combining electromagnetic induction, geophysical method by ground-penetrating radar (GPR), and acoustic detection methods. Applying the integrated detection method and considering known pipeline network designs, the properties and complex relationships of different pipeline materials (cast iron, polyethylene (PE), and polyvinyl chloride (PVC)) were determined. In addition, a spatial distribution map of the pipes from wells and the main input water supply pipelines was achieved. The results suggest that the integrated detection scheme combining these three methods provides an effective approach to analyze complex water supply pipelines in older communities, in which each single detection method has more uncertainties. The study provides valuable references for similar communities in many developing countries.

**Keywords:** urban old community; complex water pipeline system; metal pipeline detector; Ground-penetrating radar; acoustic detection

## 1. Introduction

Underground water supply pipeline systems are an integral part of urban infrastructure [1] and critical for inhabitant survival and the sustainable development of a city. Thus, the safety, stability, reliability, and efficiency of a water supply pipeline system are essential for the delivery and transmission of fresh water, maintenance of urban environments, and prevention and control of urban disasters [2–4]. Pipeline accidents frequently occur in many countries, which seriously affects people's normal work and life and can limit the development of cities and even a whole country [4]. This is especially true in developing countries, where the pipeline systems are continuously being built or reconstructed.

To maintain the normal operation of an underground pipeline system, it is critical to understand the position, direction, and distribution of underground pipelines and how these pipelines link together

in the whole three-dimensional system. However, with the prolonging of the operation periods, pipeline systems have worsened, making pipeline detection, investigations, and mapping a global task [5].

Developing countries face more pronounced pipeline problems than developed countries due to insufficient knowledge of construction technology or limited budgets. As budget often has greater importance over construction in developing countries, cheaper materials are used for pipelines [6]. Therefore, the coexistence of pipelines of different materials has largely increased the difficulty of detecting pipeline systems.

In older cities, underground pipeline systems are interlaced, and the relationships between different pipelines are complex, with the existence of some abandoned pipelines. Moreover, comprehensive maps of underground pipelines and archived management data systems are also scarce in developing countries, which may not include information about remaining pipelines. In China, older communities have always had limited budgets and limited sustainable planning for constructing pipeline systems. As the number of buildings and residents in China have sharply increased in the last 40 years, pipeline systems have expanded and become more complex, which makes it highly difficult to monitor the systems.

Many developed countries have pioneered management regulations and detection techniques for underground pipelines. For example, the United States stood as the country with the most pipeline accidents during the 1930s. By establishing legislation for pipeline safety operation, the United States constructed procedural management systems to improve pipeline safety to the greatest extent [7–9]. As such, the USA is now one of the countries with the most developed pipeline system. Switzerland has improved the condition of its “zipper road” [10,11], whereby roads are repeatedly excavated and backfilled by building an integrated underground pipe network corridor. Faced with various types of underground pipelines, different levels of ownership, and administrative management, France uses “legislation first” to regulate the responsibilities and obligations of planning, construction, operation, maintenance, and supervision of pipelines [9]. Britain takes the lead in pipeline planning and construction in urban expansion by integrating more high-tech elements into urban pipeline construction and constantly modernizing pipeline systems [10,11].

Due to the complexity of underground pipeline systems in old communities, which have had many buildings and households built in different periods, detection is very difficult and, thus, requires an urgent solution by using different technology and instruments [8,12], specifically one using integrated methods and technical flow. This study presents a mixed detection strategy by combining multiple techniques to investigate a complex underground water supply pipeline system in a typical residential community in China. We first analyzed the characteristics and current detection difficulties of the underground water supply pipeline in old urban communities. Then, we combined the electromagnetic induction, ground-penetrating radar (GPR), and acoustic detection methods into a detection scheme for the water supply pipeline. Based on theoretical knowledge of the pipeline design and estimated radar diameter in the chosen typical residential community, we successfully completed an accurate diagram of the water supply pipeline in an extremely complex area.

## 2. Characteristics of Underground Water Supply Pipelines in Old Urban Communities

### 2.1. Different Pipeline Materials

The diameter of an underground water supply pipeline is generally less than 300 mm in an old urban community in China. Common materials used to construct pipelines in China include concrete, cast iron, polyvinyl chloride (PVC), polyethylene (PE), steel belt, and hole mesh steel tape plastic composite pipe. Due to budget, construction environment, maintenance management, and other factors in the last decades, pipelines composed of various materials are connected by different methods, such as welding metal pipes directly linked to PVC pipes. However, this kind of pipeline connection makes it difficult to detect the water supply pipeline when using a metal pipeline detector alone.

## 2.2. Complexity of Pipeline Connection

The complexity of buried pipelines is mainly affected by two factors. First, the pipe network lacks long-term planning in the designing and constructing stage due to limited budget or time. At times, because limited time or conflict with other current pipelines prevents construction workers from adhering in strict accordance with the construction standards, pipe connections are not standard in some places [13]. As a result, the layouts of underground pipelines are poorly organized and difficult to detect. For example, the pipeline standard for the Chinese “Design Code for Outdoor Water Supply” (GB50013-2006) requires that the pipeline layouts should be in short and straight in order to meet the optimal hydraulic conditions. But in some old communities, the pipelines are found in a quick manner which always require the usage of more pipes, leading to problems later on. Second, new pipelines are sometimes welded directly to the existing water supply pipeline during reconstruction or when urgent repair is needed, which results in old pipelines being abandoned in the ground. This adds to the complexity of underground pipelines and causes more detection difficulties.

## 2.3. Uncertainty of Pipeline Information in Original Maps

The uncertainty of pipeline information in original maps is usually caused by three reasons. First, the various construction ages of numerous buildings in an older Chinese urban community can be a problem. Some older buildings have been renovated or expanded with the original pipeline systems, which are generally buried deeper compared to newer buildings with shallower systems. The older water supply pipelines are hidden in the interior of the building behind walls or under the building, largely increasing detection difficulty. Second, due to the long construction history of the old community, there is often no archived underground pipeline management data system. Consequently, information about underground pipelines is limited or even missing. Third reason, even the accuracy of the original maps is fine, however, the original maps have not been updated with the modification or construction of the pipelines [14]. Collectively, the lack of these basic data greatly increases the difficulty of detection.

## 3. Survey Area

### 3.1. Geographical Location

A representative old community located in the Taibai campus of Northwest University in Xi’an, Shaanxi province, China (Figure 1) with a complex pipeline system was selected for the detection experiment. The Taibai campus of Northwest University was founded in 1902 with a history of more than 110 years. Many buildings in the campus have been rebuilt and expanded during different periods, and a variety of facilities, including underground pipelines, have undergone great changes. Therefore, the water supply pipeline in this area exhibits the typical characteristics of old communities, including a large diversity of pipeline materials, complex pipeline connections, and uncertain pipeline information, which combine to make detection extremely difficult.

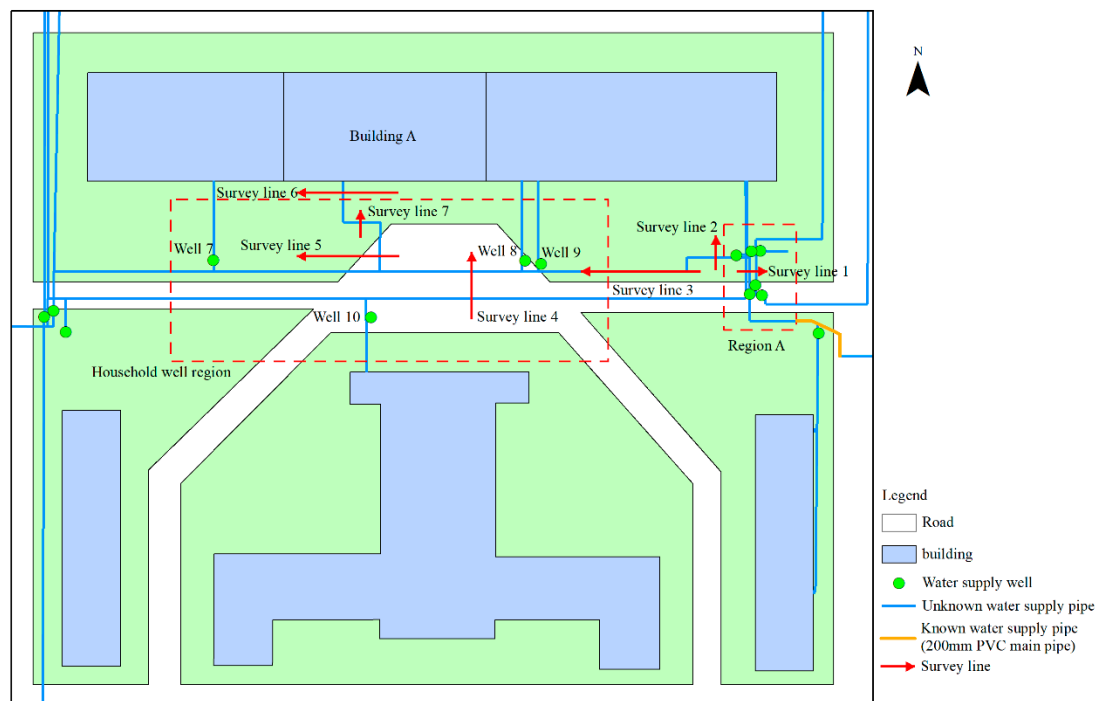
### 3.2. Survey Flow

Three basic pieces of information of underground pipelines in the survey area were obtained from the collected maps and relative background information: (1) There are two main water supply pipeline inputs from the main pipeline of the city into the study area; one is a 200-mm PVC pipe, and the other is a 100-mm or 150-mm cast iron pipe. (2) All water supply pipelines in the study area are buried less than a depth of about 2 m. (3) Except for a small section of PVC pipeline dug out during recent construction, the location, direction, and layout of all other pipelines are unknown.

The distribution of water supply wells (Figure 1) and the direction and properties of the pipelines in the wells (Table 1) were investigated. A detection scheme was then designed based on the above information.

**Table 1.** Properties of known pipelines.

Name	Diameter (mm)	Material	Burial Depth (m)
Pipe A	100	PVC (left)/cast iron (right)	0.8
Pipe B	200	PVC	1.48
Pipe C	100	cast iron	0.85
Pipe D	150	cast iron	0.65
Pipe E	150	cast iron	0.65
Pipe F	100	cast iron	0.8
Pipe G	100	cast iron	0.68
Pipe H	100	cast iron	0.8

**Figure 1.** Diagram of pipeline detection experiment in a Chinese old community.

## 4. Detection Methods and Experiment Scheme

### 4.1. Experiment Scheme

The underground pipeline system in the study area is extremely complex and has little available information. There are concentrated water supply wells in region A (Figure 1), in which the pipeline direction, material, diameter, and buried depth are variable. Although region A is complex, it has the most pipeline information, so the experimental scheme is formulated accordingly. In the experimental scheme, region A was selected as the starting point of detection, which was then expanded to the surrounding area. The inlet pipeline was detected after the main pipeline was successfully detected. The flow chart of the experiment is illustrated in Figure 2. The photo of the field work in region A is shown in Figure 3, all the known pipelines are shown in Table 1, and the type and spatial distribution of water supply wells are shown in Figure 4. The internal space of well 4 is larger than the cover, and pipe C is on the side below the well.

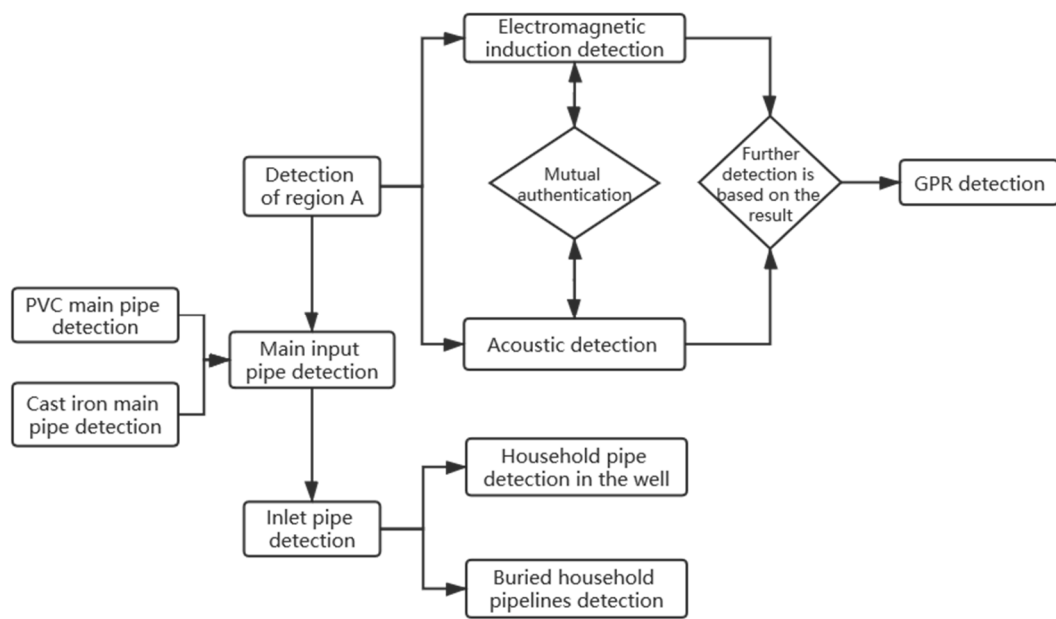
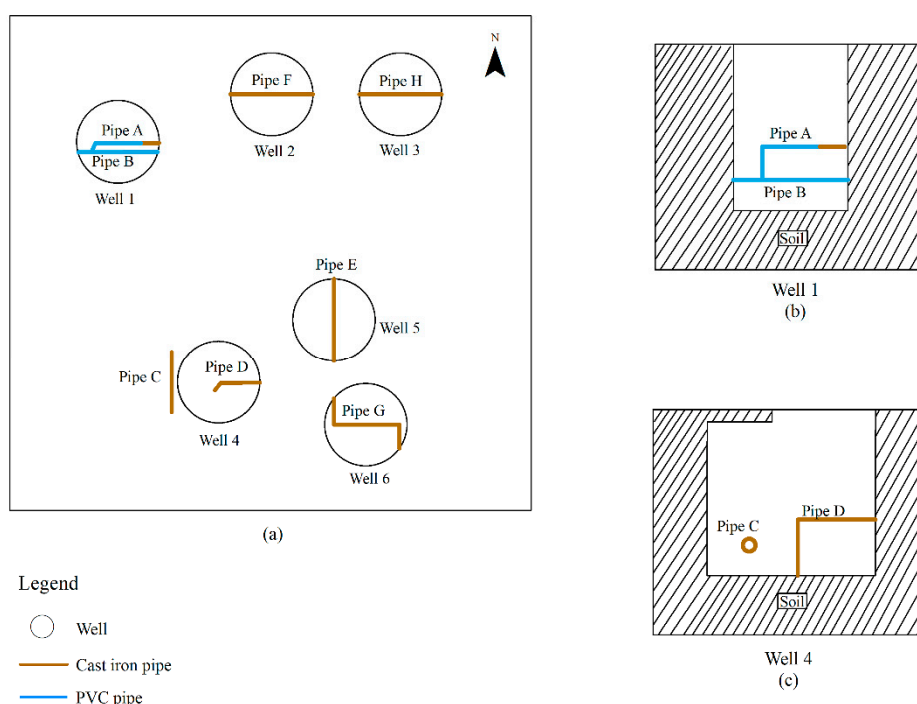


Figure 2. Experimental program flow chart.



Figure 3. Field pictures of region A.



**Figure 4.** (a) The water supply wells and pipes in the wells in region A; (b) side view of well 1; (c) side view of well 4 in experiment area.

The instruments used in this investigation included an UK Radiodetection Limited RD8100 pipeline detector, a Swedish MALAGX system GPR, stethoscope, and a hammer. The detection methods included the metal pipeline detector detection method (electromagnetic induction method), GPR, and acoustic detection. The metal pipeline detector RD8100 was utilized to detect the direction and position of the metal pipelines; the acoustic detection method was used to determine the connectivity between pipelines; and GPR identified the distribution and location of pipelines in both horizontal and vertical directions. The three methods were applied together and validated with each other via theoretical analysis.

In addition, the knowledge of the pipe network design and pipe diameter calculations from radar images were used to assist the detection process. According to the geological condition of the research area and the buried depth of the pipelines (less than 2 m), reasonable parameters of radar detection [15–20] were determined to be an antenna frequency of 450 MHz, step length of 0.025 m/ns, and time window of 46.875 ns.

#### 4.2. Methods for Underground Pipeline Detection

##### 4.2.1. The Acoustic Detection Method

The acoustic detection method was mainly used to detect metal pipes and close PVC pipes. The attenuation speed of sound waves is related to the medium—a higher attenuation rate accompanies with a softer elasticity of the medium. Because the attenuation speed of sound waves in pipelines in the ground and air are largely different, and the attenuation rate of sound waves is also related to the length and material of the pipe, the connectivity of pipes can be determined by the sound obtaining from the shells of pipes based on frequency, loudness, and tones. The sound waves attenuation rate depends on the material of the pipes and generally follows the order: steel > cast iron > concrete pipe > PE and PVC [21].

To apply this method, the hammer was banged on one side of the pipe, generating a sound source that propagated along the pipe. Then, the stethoscope was used to determine if the received oscillating sound was at the same frequency as the tapping frequency at the other side of the pipe, which indicated

if there was a direct connection or water in the pipe. This method is convenient and practical, and its accuracy is largely affected by the distance and material of the pipe. The presence of a connection can be determined, but not the direction of the pipeline, by acoustic detection method.

#### 4.2.2. The Electromagnetic Induction Method

The principle of the widely used metal pipeline detector is electromagnetic induction [22], which is based on the electrical and magnetic differences between metal pipelines and the surrounding media. A current is produced from the excitation of a transmitter and then transferred through the pipeline, and subsequently, an alternating electromagnetic field of the same frequency is generated in the surrounding space. The positions of the pipelines are then determined based on the signal received by the metal detector from the generated electromagnetic field.

Three different modes are available to connect the transmitter with the pipeline, including direct connecting, induction, and clamp connecting, among which the direct connecting mode is most commonly used.

The direct connecting mode (Figure 5) was applied to the metal pipeline by electromagnetic signals generated from the transmitter, which were collected by a receiver [23]. The direct connecting mode is also known as the charging mode and includes two connecting styles. One is the single terminal charging style (Figure 5a), which connects one of the transmitter output terminals to the pipeline and the other terminals to the grounding electrode (referred to as the infinite pole) at a position far away from the pipeline. The current passes through the pipeline with a loop between the pipeline and earth in this style. The second style is two-terminal charging (Figure 5b), in which the power supply is carried out at any two points of the pipeline, so the current forms a loop between the pipeline and transmission wire [24]. This mode requires that the pipeline must have an exposed hitch point and good grounding connection.

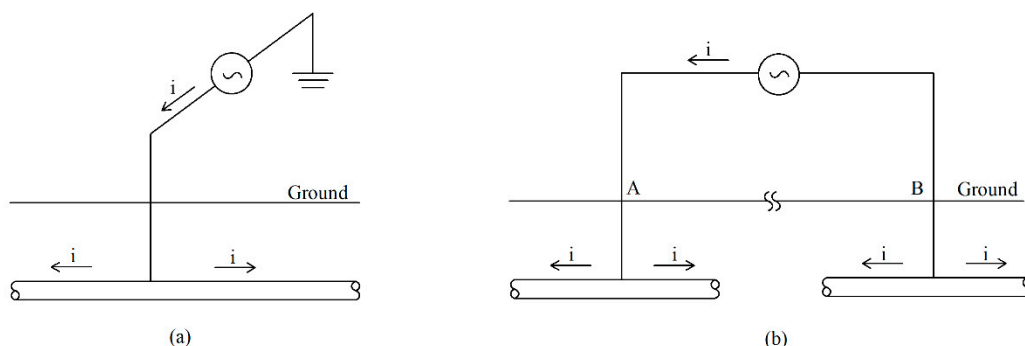


**Figure 5.** Diagram of direct connecting mode of electromagnetic induction. (a) Single terminal charging style; (b) Two-terminal charging style.

When a metal pipeline detector is used to detect complex or near pipelines, the direct connection mode of the metal detector has shown to minimize the interference of signals caused by surrounding pipelines [25]. Therefore, the direct connecting mode was selected for detection in this survey area.

#### 4.2.3. GPR

GPR uses high-frequency electromagnetic waves in the form of broadband short pulses [26] to detect underground media through excitation, transmission, reflection, and reception of signals [27–29]. The location and depth of underground pipelines can be inferred from the transmission time, amplitude, and waveform of the received wave [30]. GPR has the advantages of fast detection speed, accurate positioning, continuous scanning, data and image display [31] and can be used for both metallic and nonmetallic pipeline detection.

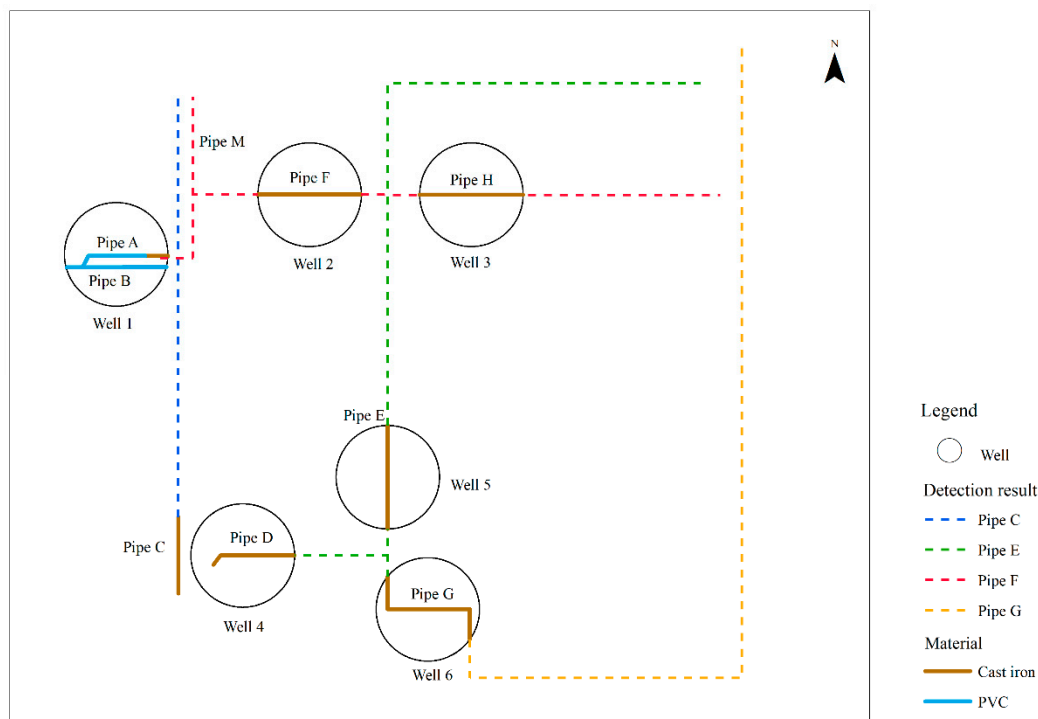
## 5. Detection Results

Figure 2 illustrates the experimental design scheme of the main pipeline to branch pipelines (known and unknown information) step-by-step, which consists of three parts. First, the most complex region, A, was explored using known information of pipelines in the wells to find the location of the main pipeline. Second, the location of the main pipeline in the research area was further investigated. Finally, the inlet pipe was detected, which includes the connection between the main and inlet pipes from the well in addition to the pipe diameter and location information of a buried inlet pipe.

### 5.1. Region A

#### 5.1.1. Electromagnetic Induction Detection Results

The metal pipeline detector was used to preliminarily investigate the pipeline system by the direct connecting mode in region A. The metal pipeline detector was connected to Pipe F in Well 2 and then probed in all directions to obtain pipeline signals. The results suggest that Pipe F connects with Pipe A and Pipe H, and there is a northbound signal between Well 1 and Well 2 in the front of the building. This proves that an inlet pipe is presented, which is marked Pipe M in Figure 6. Then, the metal pipeline detector was connected to Pipe E in Well 5, which revealed that Pipe E connects with Pipe D and Pipe G (Figure 6). When the metal pipeline detector was connected to Pipe G in Well 6, it was found that Pipe G is not connected to other pipelines in wells of region A. The connection of the detector to Pipe C in Well 4 received a pipe signal in the north of Well 4, which almost coincided with the signal of inlet Pipe M after reaching the middle of Well 1 and Well 2, but it is not connected with the pipes in Well 1 and Well 2. These results indicate that Pipe C and Pipe M are two parallel indoor pipelines that are not connected.



**Figure 6.** Schematic diagram of detection result of metal pipeline detector.



### 5.1.2. Acoustic Detection Results

The acoustic detection method was used to determine the connectivity between the pipelines and verify the results obtained by the metal pipeline detector. There are two conditions that explain why the initial tapping sound by the hammer is not received in another pipe. One obvious condition is that the two pipes are not connected. The second condition is that, even when the two pipes are connected, the sound attenuates to zero in the transmission process, for which scattering and absorption are the main processes. The scattering process occurred when the sound wave passes through an appendage such as an elbow, tee, or valve, which are always used to connect pipes, causing a sharp attenuation. The absorption process occurred when sound waves are converted into heat during propagation and absorbed by the medium, and they decay as the propagation distance increases. When there are too much appendages or too long pipes between the two pipes, sound waves decay to zero as they travel by pipes. Considering that area of region A in this old community is only about 40 m<sup>2</sup>, the sound waves cannot be attenuated to zero in cast iron or PVC pipes at such short distances. Thus, the reason for no received signal is due to the pipes not being connected to each other.

The experimental results (Table 2, Figure 7) of acoustic detection suggest that (1) Pipe A, Pipe F, and Pipe H are connected; (2) Pipe D, Pipe E, and Pipe G are connected; (3) Pipe B is connected to Pipe D but not directly connected with Pipe E and Pipe G; and (4) Pipe C is not connected to any pipes in region A. The current detection results confirm the connectivity between pipelines but cannot accurately suggest the direction and position of the underground pipelines.

**Table 2.** The experimental results of the acoustic detection method.

Origin of Generated Sound	Test Well/Pipeline	Response	Connection Relationship
Well 1 Pipe A	Well 2 Pipe F	1	Pipe A, Pipe F and Pipe H are connected.
	Well 3 Pipe H	0	
Well 1 Pipe B	Well 2 Pipe F	0	Pipe B is not directly connected with Pipe F and Pipe H
	Well 3 Pipe H	0	
Well 4 Pipe D	Well 5 Pipe E	1	Pipe D, Pipe E and Pipe G are connected
	Well 6 Pipe G	1	
Well 4 Pipe D	Well 5 Pipe E	0	Pipe C, Pipe E and Pipe G are connected
	Well 6 Pipe G	0	
Well 4 Pipe C	Well 1	0	There is no direct connection between Pipe C and pipes in Well 1 and Well 2
	Well 2 Pipe F	0	
Well 4 Pipe D	Well1 Pipe A	1	Pipe A is connected to Pipe D through Pipe B
	Well1 Pipe B	1	
Well 5 Pipe E	Well1	0	The pipes in Well 5 and Well 6 are not directly connected with those in Well 1 and Well 2
	Well 2 F	0	
Well 6 Pipe G	Well 1	0	
	Well 2 F	0	

Note: The response column indicates whether there is vibration sound in the pipeline with the same frequency as the sound source, where 1 is yes, and 0 is no.

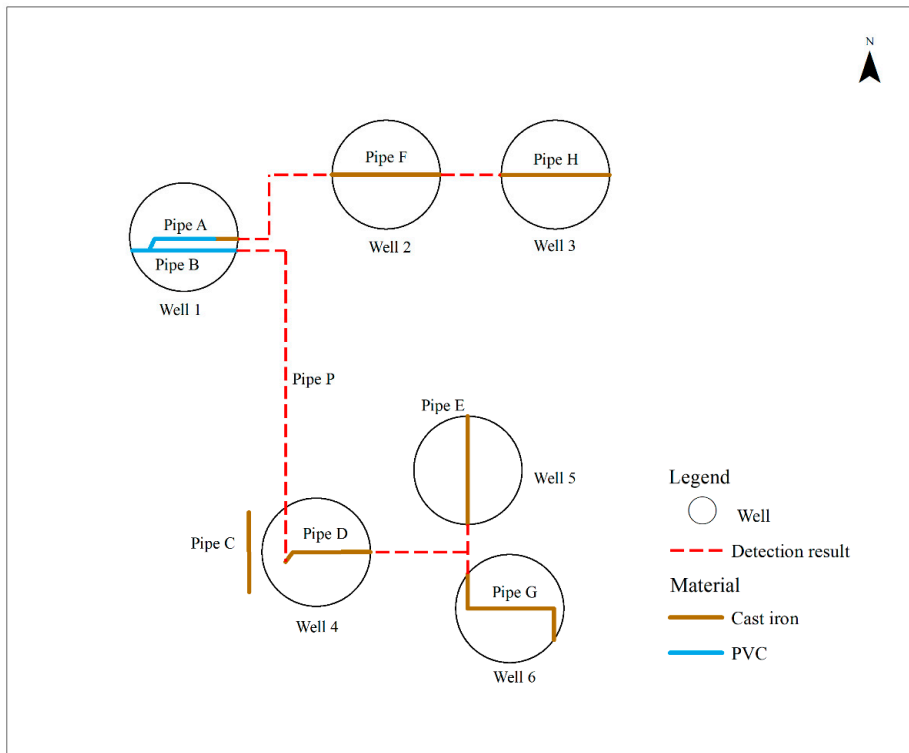


Figure 7. Schematic diagram of acoustic method detection results in the region A of the old community.

By comparing Figures 6 and 7, it can be suggested that, except for Pipe P, the detection results of the metal pipeline detector are consistent with those of the acoustic detection method, which further proves the accuracy of the detection results of the metal pipeline detector. The result diagram in Figure 8 was drawn based on the current detection results.

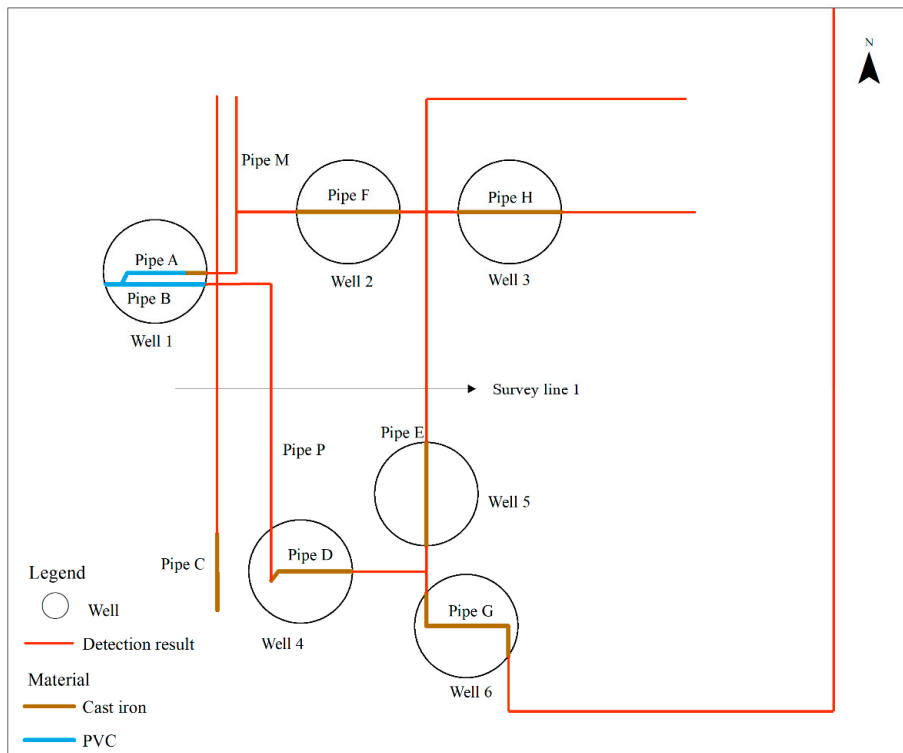
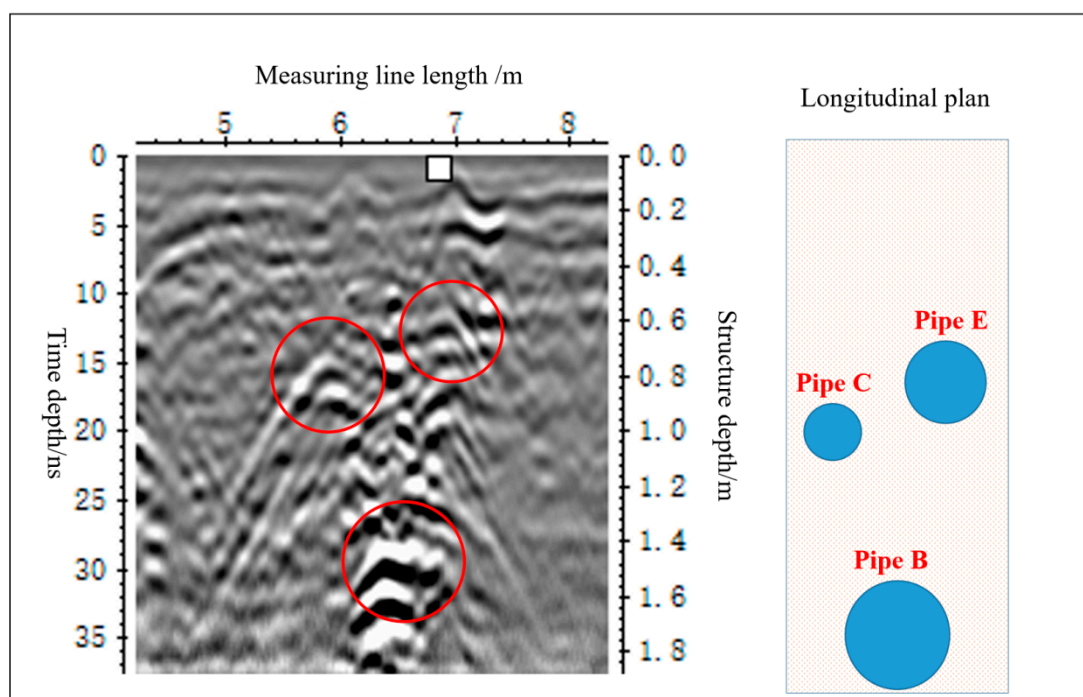


Figure 8. Schematic diagram of detection results in the region A of the old community.

### 5.1.3. GPR Detection Results

GPR was used to determine the position and direction of PVC pipes in region A. The following information had obtained before the GPR survey: Pipe B is a 200-mm PVC main pipe; Pipe D is a 150-mm cast iron pipe; and Pipe B is connected to Pipe D. However, the connection signal between Pipe B and Pipe D cannot be detected by the metal pipeline detector. It is speculated that there is a 200-mm PVC Pipe P (Figure 7) that connects Pipe B with Pipe D, so we used the GPR to verify this assumption. It can be seen that there are multiple strong abnormal reflection waves between 5.2 and 7.4 m from the detection starting point (Figure 9). Between the distance of 6.2 and 6.8 m from the detection starting point at a depth of about 1.4 m, there is an electromagnetic wave diffuse reflection phenomenon, which is indicative of uneven soil [32]. There are some reflection waves in Structure depth 0.0–0.2 m and 7 m in line length, which is caused by heterogeneous material of the soil. Although the phenomenon causes interference to the radar image, three abnormal reflection waves with a hyperbolic shape can be clearly seen in Figure 9, correlating to pipeline reflection curves at 5.9, 6.4, and 6.9 m from the detection starting point.



**Figure 9.** Radar image of survey line 1 in the region A in the old Taibai campus of Northwest University.

Because cast iron pipes present a shielding effect to electromagnetic waves, the radar image displays multiple reflections under a parabola. However, these reflections are not always obvious and have no effective information about the strata under the cast iron pipe because it also could be obtained due to the shielding effect. The top of the parabola of cast iron pipes is usually white and black, where the black phase axis is often more prominent than those in radar images of other types of pipes [33].

Comparatively, it is easier to obtain clear images via GPR of PVC pipelines since they are non-metallic. The radar image shows the abrupt changes between black and white color at the same axis, which provides information about the position and depth of pipes. This is based on the wave theory, where the vibration direction of the wave is opposite to the direction that the wave propagates and is equivalent in distance to half the wavelength [34–36]. The electromagnetic wave emitted by GPR travels through the stratum and does not reverse the phase when it encounters a non-metallic pipeline [37]. In addition, as the non-metallic layer has no shielding effect, the effective information in the layer below the pipeline can be illustrated in the radar image [32,33].

The top curves at 5.9 m and 6.9 m from the starting point alternate between black and white (Figure 9). The multiple reflection waves under the curve indicate that the two abnormal curves are metal Pipes C and E, respectively. The buried depths of Pipe C and Pipe E are 0.8 and 0.65 m, which displayed as bright points near the radar survey lines at 0.85 and 0.65 m, respectively. The results are consistent with the acoustic detection results, and the slight differences are caused by variations in the topography.

At the top of the parabola, which is 6.3 m from the starting point, the alternating colors of black and white in the image suggest the presence of PVC Pipe P. The detection depth of the target Pipe P is 1.46 m, while the buried depth of PVC Pipe B directly connected to Pipe P is 1.48 m (Table 1). The detection results indicate that the main pipes in this section do not bend up or down and their buried depth only varies slightly with local topographic relief.

## 5.2. Main Input Pipeline Detection

### 5.2.1. Main Input PVC Pipeline Detection

After part of the main input PVC pipeline in region A was determined, several radar survey lines were arranged (Figure 10). The abnormal curve of the hyperbolic shape in survey line 2 indicates there is a main PVC pipe (Figure 10a). The parallel abnormal waves with alternating black and white color at 4 m from the detection starting point to the end of survey line 2 suggest that the PVC pipe has secondary reflection (Figure 10b). The anomalous wave occurred because the radar line was placed directly above and parallel to the main PVC pipe; thus, the parallel reflection waves of the two black layers are the reflection waves of the top and bottom of the PVC pipe. Multiple abnormal curves in survey line 4 are displayed in Figure 10c, in which the anomaly in the left red box suggests a thermal pipe trench. The abnormal curve at 8 m with a detection depth of 1.44 m indicates a main PVC pipe.

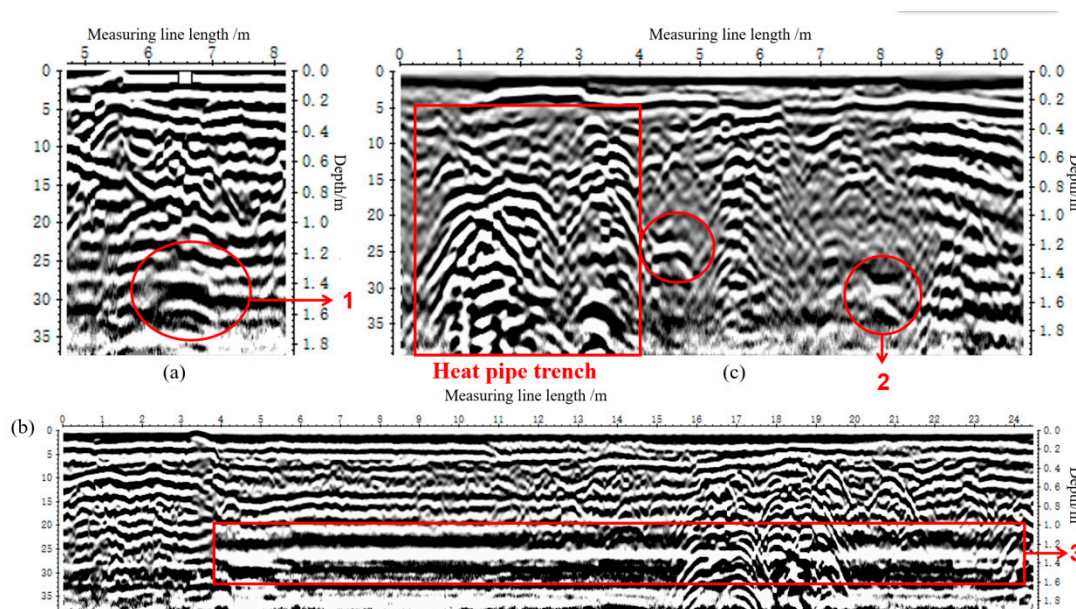


**Figure 10.** Radar image of (a) survey line 2; (b) survey line 3; (c) survey line 4 in the region A of the old community.

### 5.2.2. Main Cast Iron Pipe

While the metal pipeline detector was directly connected to Pipe C of Well 4, the result reveals that the water supply pipeline turned to the west at 0.5 m south of Well 4. The direction of the pipeline did not change until the end of the road, where it then connected to another north-south main pipeline. The detection suggests that this is the main cast iron pipe in the study area and has a diameter of 100 mm.

A parabola shape at a distance of 4.5 m from the detection starting point can be observed in Figure 10c, although it is not obvious due to the influence of the nearby thermal pipe trench. It can be determined that there is a pipe at this position at a detection depth of 0.96 m. The radar detection result is consistent with that obtained by metal pipeline detection, indicating that this pipe is the main cast iron pipe. Moreover, 1, 2, and 3 in Figure 10 are radar pipeline images of the same PVC main pipeline in different positions at different sections.

### 5.3. Inlet Pipe Detection

Relevant information shows that there are five inlet pipes connected with main input pipelines outside region A. All inlet pipes are cast iron, among which four pipes are in water supply wells and one is directly buried that enters the house. The buried pipe mainly supplies water to building A, but its diameter and direction are unknown and need to be determined.

#### 5.3.1. Inlet Pipe from Wells

The four inlet wells in the study area are marked as Well 7, Well 8, Well 9, and Well 10. While the metal pipeline detector was connected to Pipe C in Well 4, the detection results suggest that the pipe in Well 10 connects to the main input cast iron pipeline, but the pipes in Well 7, Well 8, and Well 9 are not connected to this main pipeline. In addition, when the metal pipeline detector was connected to the pipes in Well 7, Well 8, and Well 9, the pipeline signal disappeared within a certain distance in south of the well where the pipelines are located. This specific location is exactly where the main PVC pipe is. Thus, the results indicate that the pipes in Well 7, Well 8, and Well 9 are connected to the main PVC pipe.

Then, the acoustic detection method was used for validation. When the pipe in Well 8 was knocked with the hammer, the sound was clearly heard through the pipe in Well 9, which confirms that pipes in Well 8 and Well 9 connect with the same main pipe. The pipe diameter of Well 9 is 150 mm, the diameter of the main cast iron pipe is 100 mm, and the main PVC pipe diameter is 200 mm. According to the pipe design specification, the diameter of the indoor pipe should be smaller than the main pipe that it connects to. Considering that the pipe in Well 9 is connected to the main PVC pipe, the pipe in Well 8 is also connected to the main PVC pipe. The above detection results and logistic analysis suggest that Well 7 is connected with the cast iron pipe, and Well 8, Well 9, and Well 10 are connected with the main PVC pipe.

#### 5.3.2. Buried Inlet Pipeline

The water consumption [38–40] needs to be known to estimate the diameter of the buried inlet pipe that supplies water to building A. The main consumers in building A include some shops in the front rooms and a school canteen, with water primarily supplying bathrooms and kitchens. According to the number of investigated plumbing fixtures (Tables 3 and 4), the water consumption of building A was estimated using formulas (1–3) and the relevant parameters, which were selected according to China's building water supply and drainage design specifications.

**Table 3.** Water consumption statistics of bathroom appliances.

Plumbing Fixture	Number of Fixtures (a)	Flow Rate (L/S)	Percentage of Simultaneous Water Supply
Pedestal pan	2	0.10	50
Squatting pan	12	1.20	50
mop tub	9	0.15	60
urinal	5	0.10	50
washbasin	10	0.15	60

**Table 4.** Statistics of water consumption of kitchen appliances.

Kitchen Fixture	Number of Fixtures (a)	Flow Rate (L/S)
Single sink table	10	0.15
Hand wash sink Cabinet	5	0.15
Big wok rang	7	0.10
wok rang	7	0.10
Drain type soup stove	7	0.20
1-door steam cabinet	8	0.20
Hookah hood control box	8	0.10
3-head noodle cooker	7	0.15
Bain marie cabinet	10	0.20
Water heater	10	0.20
Big single sink table	8	0.20
Reel kleen unit	8	0.20

$$Q_1 = \sum q_o \times n_o \times b \quad (1)$$

$$Q_2 = \eta \times \sum q_o \times n_o \quad (2)$$

$$Q = Q_1 + Q_2 \quad (3)$$

where  $Q$  is the total water consumption used for toilets and kitchen appliances;  $Q_1$  is the total water consumption for toilet fixtures;  $Q_2$  is the total water consumption for kitchen fixtures;  $q_o$  is the nominal flow;  $n_o$  is the number of plumbing fixtures;  $b$  is the percentage of simultaneous water supply; and  $\eta$  is the percentage of simultaneous water supply, which is taken as 75% [41–44].

The total water consumption for bathroom fixtures was determined to be 9.26 L/S using formula (1). The total water consumption for kitchen fixtures was estimated as 11.78 L/S via formula (2). The total water consumption of building A is 21.04 L/S estimated by formula (3).

Then, the diameter of the water supply pipe was calculated using the following equation:

$$D = \sqrt{\frac{4Q}{\pi v}} \quad (4)$$

where  $D$  is the diameter;  $Q$  is the flow; and  $v$  is the flow rate of 1.5 m/s.

The calculated diameter of the indoor pipe is 134 mm. In the design of the pipeline, the diameter of the pipeline will be selected from the existing diameter specifications, which is equal to or a little bigger than the calculated diameter in the Chinese water supply and drainage design manual. The calculation suggests the diameter of the inlet pipe should be at least 150 mm, but no more than 200 mm according to the specification of the pipe. Thus, the inlet pipe should connect to the main input PVC pipe, which have equal diameters.

In order to determine the exact location of the pipeline, several parallel GPR survey lines in front of building A were arranged (Figure 11). Except for a known sewage pipe and a target water supply pipe, all the pipes passing through the area are abandoned pipelines. The hyperbola at 18.2 m in Figure 11a and 19 m in Figure 11b suggest the same sewage pipe. The abnormal wave in hyperbolic form at 9.4 m may be the target water supply pipe, marked as suspicious pipe 1, with a detection depth of 1.6 m and distance of 9.6 m from the known sewage pipe (Figure 11a).

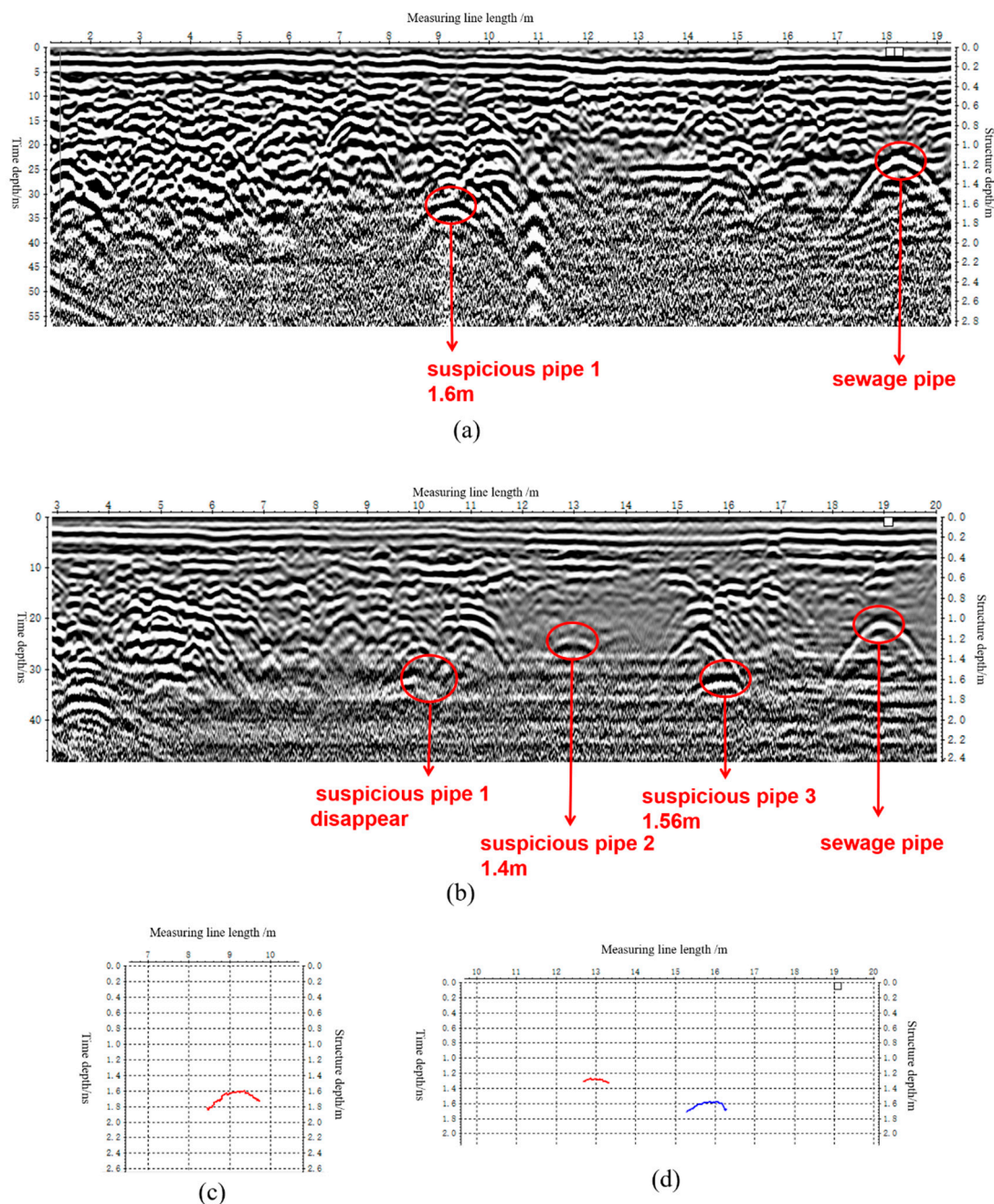


**Figure 11.** (a) Radar image of survey line 5; (b) Radar image of survey line 6; (c) Image of the extraction point of suspicious pipe 1; (d) Image of the extraction point of suspicious pipe 2 and suspicious pipe 3 from left to right.

The pipeline at 9.6 m from the known sewage pipe disappears, and hyperbola abnormal waves appear at 13 and 16 m (Figure 11b), respectively. They were marked as suspicious pipe 2 and suspicious pipe 3. Among these, there should be at least one water supply pipeline. It is assumed that the water supply pipeline changed its direction between survey line 5 and survey line 6 (Figure 1). To further determine the target water supply pipeline, the pipe diameter of the suspicious pipeline in the radar image was calculated.

The hyperbolic curves of the suspicious target water supply pipeline in GPR images of survey lines 5 and 6 were extracted by Reflexw post-processing software [45]. The extraction position of suspicious pipe 1 was estimated from Figure 11c, while the extraction positions of suspicious pipe 2 and suspicious pipe 3 from left to right can be estimated from Figure 11c,d, respectively. The extraction

point was fitted with the parabola to determine the diameters of the pipes [46–48]. The diameter of suspicious pipes 1, 2, and 3 were calculated as 150, 250, and 150 mm, respectively. According to China's building water supply and drainage design specifications, the target water supply pipe's diameter should not be changed. The diameter of the target water supply pipelines is 150 mm or 200 mm, so suspect pipes 1 and 3 are the target water supply pipelines. The inflection point of the water supply pipeline can be found in survey line 7 (Figure 12), in which the abnormal curve with hyperbolic shape at 0.5 m is considered the target water supply pipe.

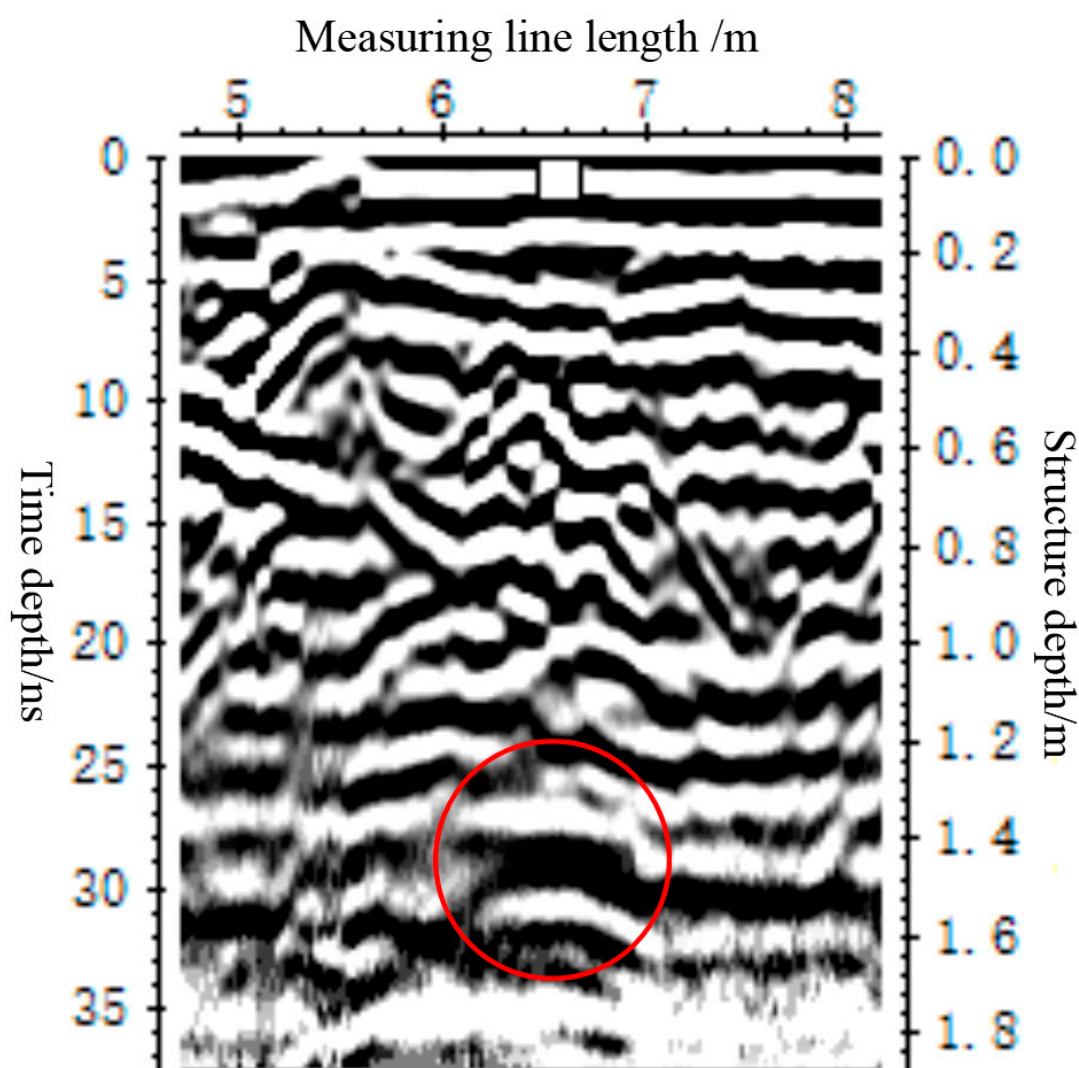


Figure 12. Radar image of survey line 7 in region A of the old community.

## 6. Discussion

We introduced an integrated pipeline detection scheme in an old community in China with complex pipeline layouts. Our results suggest that the pipeline detection should start from the open place such as well, and then expand to around pipelines. The detection results obtained from different methods at each step probably get parts of new information of pipelines, and the uncertainty in detection can be reduced on step by step, and the spatial distribution of the whole pipelines can be obtained through the integrated analysis of the detection results of each step.

The exploration in this study suggested that the three detection methods have their own advantages and limitations. It can be summarized as follows: electromagnetic induction method has the advantage on “the trend of metal pipe”; acoustic detection has the advantage on “whether the pipe is connected”;



geological radar has the advantage on “does the pipe exist there.” When using a certain method alone, their limitations are exposed: metal pipeline detectors cannot detect non-metallic pipelines, and are susceptible to the interference of magnetic field which caused by magnetic objects like iron pillars, mutual interference between different types of pipelines and so on. The use of acoustic detection method which cannot track and locate pipelines is limited by the exposed condition and distance of the pipeline. The detection effect of GPR which also cannot track pipelines is greatly affected by the underground medium [49]. It can be seen that, in the face of the unknown and complicated underground pipeline world, it is difficult to solve the practical problems only by using a single method, which sometimes even cannot guarantee the accuracy of detection result, so the existing methods need to be used together. In practical application, according to the urgent pipeline problems to be solved, the detection methods with corresponding advantages are preferred, and other methods are used to assist or verify, which can quickly and accurately solve most of the pipeline detection work.

GPR detection was served as a proof-of-concept method by arranging multiple radar survey lines, the target pipeline can be determined effectively after finding appropriate references and comparing and analyzing multiple radar detection results. The radar detection test in of the main pipeline suggested that when there are no more other pipelines in the detection area, it is very effective to obtain the buried depths of pipeline.

The indoor pipeline detection experiment suggested that when there are other interfering pipelines in the detection area, it must consider the known pipelines and the buried depth as a reference, the target pipeline among several pipes can be identified at first. If the pipe diameter of the target pipeline is known, GPR survey is a very useful method to calculate the pipe diameter through radar images. Furthermore, the indoor pipeline detection experiment also suggests that according to the water consumption, the feeding pipe can be estimated with the knowledge of pipe network design. In this study, pipeline network design knowledge and radar image pipe diameter calculation are creatively applied to pipeline detection. In the past, the idea of pipeline detection was to find out the existing pipeline. Based on this, this method calculated the pipe diameter of the target pipeline from the perspective of pipe network design and determined the target pipeline from the suspicious pipeline according to the conditions of pipe diameter change and successfully completed the pipeline detection.

Therefore, in order to successfully carry out pipeline detection, the selection and cooperation of detection methods, none of which are all dispensable.

In order to prove the reliability of acoustic detection, a verification experiment was designed. Based on the principle that the shear waves of sound waves cause particles to vibrate up and down during propagation, a simple acoustic amplifier (Figure 13) was made [50]. When the sound wave is transmitted to the pipe where the device is located, the device can further reflect the connection of the pipe by visualizing the sound wave through the fluctuation of water surface. A simple acoustic amplifier is attached to the pipe, and the surface of the water remains relatively still after a period of time without striking the pipe. The water flow in the water pipe causes little vibration, which is not enough to affect the water surface of the amplifier. When the detected pipe is disconnected to the knocked pipe, no tapping sound can be heard through the stethoscope, and the water remains still. When the detected pipe connected to the knocked pipe, tapping sound in the pipe can be heard through the stethoscope, and the water surface fluctuates obviously. After many tests, it is found that the pipelines in the survey area meet the requirements of acoustic detection, which indicates the results of acoustic detection in the survey area are reliable.

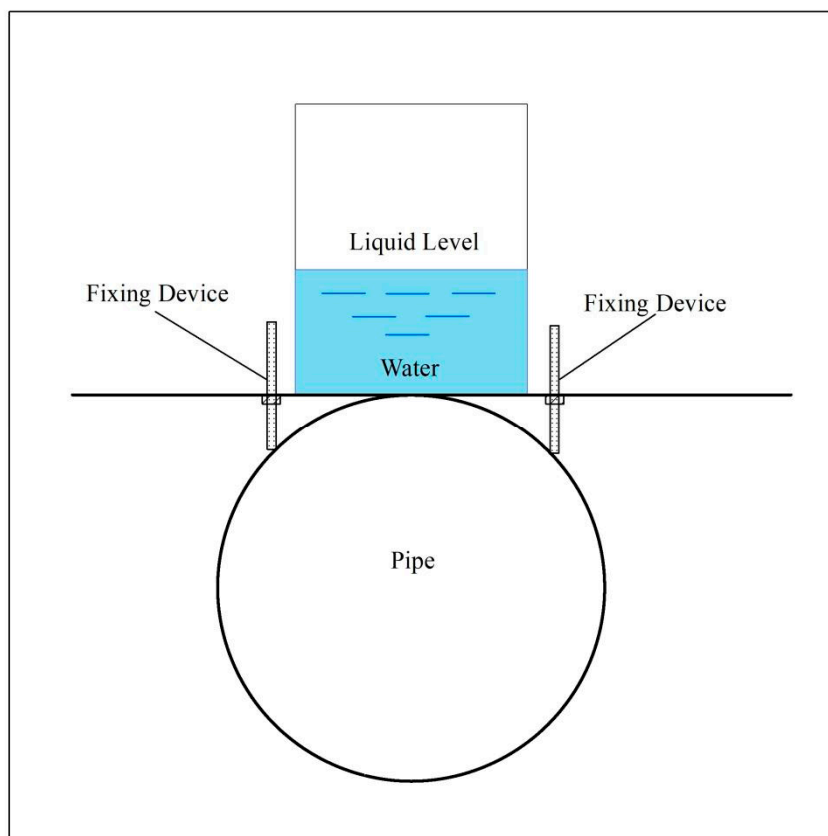


**Figure 13.** Schematic diagram of simple acoustic amplifier experiment.

There are also some limitations in the study. First, this study only focused on how to mix these methods but did not conduct in-depth research on a specific method in theory. Second, in various radar experiments, if there are unknown interferential pipelines, or the pipe diameter of the target pipeline cannot be obtained, or the pipe diameter calculated by several suspicious pipelines is the same, how to determine the depth and diameter of the target pipeline is still need to further exploration. Moreover, due to the high requirement of radar image quality, not all pipes' radar images could be used to calculate the pipe diameter. The clearer and more complete the curve presented by the pipe in the radar image, the higher the accuracy of pipe diameter calculation results. The radar pipeline image information in Figures 10 and 11 is incomplete and unclear, which is not suitable for pipe diameter calculation. It is significant to study the related problems about the pipe diameter calculation of radar image. Acoustic detection method judged the sound mainly from the pipeline; however, electromagnetic induction probably interpreted the signal. What is more, the acoustic sounding method and high-precision acoustic amplifier can judge the water flow in the pipeline [51–54], which is worth further exploration. As the water supply system standard and the measures of water saving and the development stages vary between countries, the water consume estimation method should be adjusted according local conditions, and its accuracy needs to be further explored [38,40].

In this scheme, the three detection methods are not new, and the detection instruments are common. In practice, however, it highly decreased the uncertainty of detection by integrating the results of three method and other assist knowledge in the old community, in which the water supply system is very complicated. We successfully applied the integrated methods and skills to detect all the pipelines in the Taibai campus of Northwest University in 2019, which indicates that it has good potential to be applied to other old communities.

## 7. Conclusions

Detection of underground pipeline is a multi-field, multi-disciplinary work. In view of the particularity and complexity of water supply pipelines in old urban communities in developing countries, a detection experiment was designed and tested in one typical old community in Xian, China. The following conclusions can be made:

1. The acoustic detection method is advantageous in detecting the connectivity between pipes, while the electromagnetic induction method is better at detecting metal pipes. GPR is more effective at detecting both metal pipes (cast iron) and plastic pipes (PE and PVC pipes). However, there are more uncertainties when only using one method alone.
2. The acoustic detection method, electromagnetic induction method, GPR method, and knowledge of water consumption can be integrated to validate each other when detecting the position and diameter of complex underground water supply pipelines in the old community.
3. Abandoned interferential pipes are the most difficult to be detected in old communities. They require more time to analyze the relationships between different pipes.

**Author Contributions:** Conceptualization, S.D.; Data curation, S.D.; Funding acquisition, S.Z.; Investigation, S.D., S.M., and X.Z.; Methodology, S.D., S.M., X.Z., and S.Z.; Resources, X.Z.; Software, X.Z. All authors have read and agreed to the published version of the manuscript

**Funding:** The National Natural Science Foundation of China: 41730751

**Acknowledgments:** This work was supported by the National Natural Science Foundation of China (41730751).

**Conflicts of Interest:** The authors declare no conflict of interest.

## References

1. Lai, W.W.-L.; Dérobert, X.; Annan, P. A review of Ground Penetrating Radar application in civil engineering: A 30-year journey from Locating and Testing to Imaging and Diagnosis. *NDT E Int.* **2018**, *96*, 58–78.
2. Song, Z. Study on Urban Underground Pipeline Planning and Management in China. Master Dissertation, Jilin University, Jilin, China, 2008. Available online: <https://kns.cnki.net/KCMS/detail/detail.aspx?dbcode=CMFD&dbname=CMFD2008&filename=2008063704.nh&v=MDkwNTBSdEZ5RGdXcnJLVjEyN0ZyTytZGJNcTFVFYlBJUjhlWDFMdxhZUZdEaDFUM3FUcdNMUZyQ1VSN3FmWmU=> (accessed on 8 December 2019).
3. Song, K. Analysis of Current Situation and Development Trend of Underground Pipeline Detection in China. *Tech. Innov. App.* **2017**, *35*, 184–186.
4. Canto-Perello, J.; Curiel-Esparza, J. An analysis of utility tunnel viability in urban areas. *Civ. Eng. Environ. Syst.* **2006**, *23*, 11–19. [[CrossRef](#)]
5. Ryder, A.A. International Conference on Pipelines and the Environment, held at the Royal Bath Hotel, Bournemouth, England, UK, during 8–10 March 1988. *Environ. Conserv.* **1988**, *15*, 279. [[CrossRef](#)]
6. Li, H. Research Progress of Urban Underground Pipeline Detection and Management Technology. *Resource Info. Eng.* **2018**, *33*, 142–143.
7. Perry, W.D.; Haynes, K.E. Prioritizing Regulatory Policy in Pipeline Safety. *J. Contingencies Crisis Manag.* **1993**, *1*, 90–100. [[CrossRef](#)]
8. McGrawHill. Incorporated. Pipelines Need Urgent Action. *Eng. News-Record* **2000**, *224*, 47.
9. Fandrich, D. Pipeline Industry Unites To Urge Passage Of Pipeline Safety Legislation. *Pipeline Gas J.* **2001**, *228*, 4.
10. Wiggins, L. Development of an England-wide nursing director talent pipeline. *Nurs. Manag. (Springhouse)* **2018**, *49*, 51–53. [[CrossRef](#)]
11. Xu, A.; Jiang, H.; Wei, Z. How to Build and Manage the Underground Pipe Network Overseas. *China Constr.* **2018**, *11*, 32–35.
12. Johnson, F. Introduced about 25 years ago in England, ‘pipe-bursting’ is just now gaining acceptance in Utah. *Enterprise/Salt Lake City* **2007**, *36*, 52.
13. Xie, Z.; He, J.; Hou, Z. Analysis and Countermeasures of Existing Problems in Urban Underground Pipeline Management. *Informatiz. China Constr.* **2018**, *23*, 52–55.

14. Chen, Q. Analysis of Problems and Countermeasures in the Construction of Urban Underground Pipe Network. *Intell. Build. Smart City* **2018**, *8*, 98–99.
15. Tillard, S.; Dubois, J.C. Analysis of GPR data: wave propagation velocity determination. *J. Appl. Geophysics* **1995**, *33*, 77–91.
16. Van Kempen, L.M.; Sahli, H.; Brooks, J.; Cornelis, J. *New Results on Clutter Reduction and Parameter Estimation for Land Mine Detection using GPR*; SPIE-Intl Soc Optical Eng.: Vancouver, BC, Canada, 2000; Volume 4084, pp. 872–879.
17. Pettinelli, E.; Vannaroni, G.; Di Pasquo, B.; Mattei, E.; Di Matteo, A.; De Santis, A.; Annan, P.A. Correlation between near-surface electromagnetic soil parameters and early-time GPR signals: An experimental study. *Geophysics* **2007**, *72*, A25–A28. [[CrossRef](#)]
18. Chiarabba, C.; Moretti, M. An insight into the unrest phenomena at the Campi Flegrei caldera from  $V_p$  and  $V_p/V_s$  tomography. *Terra Nova* **2006**, *18*, 373–379. [[CrossRef](#)]
19. Pennock, S.; Jenks, C.; Orlando, G.; Redfern, M. *In-pipe GPR Configuration and the Determination of Target Depth and Ground Permittivity*; Institute of Electrical and Electronics Engineers (IEEE): Piscataway, NJ, USA, 2012.
20. Xie, F.; Wu, C.G.-W.; Lai, W.W.-L.; Sham, J.F.C. Correction of multi-frequency GPR wave velocity with distorted hyperbolic reflections from GPR surveys of underground utilities. *Tunn. Undergr. Space Technol.* **2018**, *76*, 76–91. [[CrossRef](#)]
21. Wen, J.; Bu, S.; Zhang, L.; Huang, X.; Zhang, Y. Research on the Location of Leakage Points in Metal Water Pipes Based on Attenuation Characteristics of Leakage Sound Waves. *Coll. Phys.* **2013**, *32*, 29–32.
22. Wang, G.F. On underground pipeline census work method. *World Nonferrous Met.* **2016**, *24*, 47–49.
23. Du, L.; Li, X. Application of Fdetection Techniques of Underground Pipelines under Complicated Conditions. *Geol. Prospect.* **2007**, *3*, 116–120.
24. Zhao, X.J.; Zhuo-He, W.U. The Effectiveness of Several Methods for Detection of Short-interval Parallel Pipelines. *Geophys. Geochem. Explor.* **2004**, *42*, 17–21.
25. Meng, W. Discussion on Underground Comprehensive Pipeline Detection in Urban Communities. *Beijing Surv. Mapp.* **1998**, *01*, 29–32.
26. Wang, L.; Zheng-Wen, L.I.; Wang, X.B. A study of Gedological Radar to cavern detection and physical analogue. *Prog. Geophys.* **2008**, *23*, 280–283.
27. Roberts, R.L.; Daniels, J.J. Modeling near-field GPR in three dimensions using the FDTD method. *Geophysics* **1997**, *62*, 1114–1126. [[CrossRef](#)]
28. Hua, L.I.; Guang-Yin, L.U.; Xian-Qi, H.E.; Deng, K. The progress of the GPR and discussion on its future development. *Progress Geophys.* **2010**, *25*, 1492–1502.
29. Meschede, M.; Asprion, U.; Reicherter, K. Visualization of tectonic structures in shallow-depth high-resolution ground-penetrating radar (GPR) profiles. *Terra Nova* **1997**, *9*, 167–170. [[CrossRef](#)]
30. Cai, W. Exploration of Underground Pipeline Detection Technology under Complex Condition. *Low Carbon World* **2016**, *29*, 109–110.
31. Grasmueck, M.; Weger, R.; Horstmeyer, H. Full-resolution 3D GPR imaging. *Geophysics* **2005**, *70*, K12–K19. [[CrossRef](#)]
32. Grote, K.; Anger, C.; Kelly, B.; Hubbard, S.; Rubin, Y. Characterization of Soil Water Content Variability and Soil Texture using GPR Groundwave Techniques. *J. Environ. Eng. Geophys.* **2010**, *15*, 93–110. [[CrossRef](#)]
33. Zhang, J.; Cong, X.; Yang, B.; Wang, X.; Liu, Y.; Li, X. Characteristics Analysis of Radar Map on Underground Pipeline Detection. *Progress Geophys.* **2018**, *34*, 1–8.
34. Electromagnetic Wave Theory. *Phys. Today* **1955**, *8*, 33. [[CrossRef](#)]
35. Rowan, D.J.; Kalff, J.; Rasmussen, J.B. Estimating the Mud Deposition Boundary Depth in Lakes from Wave Theory. *Can. J. Fish. Aquat. Sci.* **1992**, *49*, 2490–2497. [[CrossRef](#)]
36. Berkhout, A.J.; Verschuur, D.J. Estimation of multiple scattering by iterative inversion; Part 1, Theoretical considerations. *Geophysics* **1997**, *62*, 1586–1595. [[CrossRef](#)]
37. Ayala-Cabrera, D.; Herrera, M.; Izquierdo, J.; Pérez-García, R.; Fernandez, M.H. Location of buried plastic pipes using multi-agent support based on GPR images. *J. Appl. Geophys.* **2011**, *75*, 679–686. [[CrossRef](#)]
38. Li, K.; Ma, T.; Feng, Y.; Feng, X. Urban Industrial Water Supply and Demand: System Dynamic Model and Simulation Based on Cobb–Douglas Function. *Sustainability* **2019**, *11*, 5893. [[CrossRef](#)]
39. Liu, Y.; Tao, Z.; Yang, J.; Mao, F. The Modified Artificial Fish Swarm Algorithm for Least-Cost Planning of a Regional Water Supply Network Problem. *Sustainability* **2019**, *11*, 4121. [[CrossRef](#)]

40. Nakagawa, Y. Taking a Future Generation's Perspective as a Facilitator of Insight Problem-Solving: Sustainable Water Supply Management. *Sustainability* **2020**, *12*, 1000. [[CrossRef](#)]
41. Peng, S. Discussion on the parameter value of calculation formula of hot water system for class III dormitory. *Water Wastewater Eng.* **2012**, *48*, 110–111.
42. Li, L.; Zhang, P. Tianjin Olympic aquatic center water supply system design. *Water Wastewater Eng.* **2008**, *12*, 83–86.
43. Zhao, Q. Design and debugging of water supply system for students' dormitory in boarding school. *Water Wastewater Eng.* **2013**, *49*, 84–86.
44. Zhao, Q.; Ma, B.; Li, W. Some Opinions on "Discussion on Water Supply Calculation Formulas of New Boarding Institutions in Shanghai". *Water Wastewater Eng.* **2005**, *11*, 79–81.
45. Terrasse, G.; Nicolas, J.-M.; Trouvé, E.; Drouet, E. Application of the curvelet transform for pipe detection in GPR images. In Proceedings of the 2015 IEEE International Geoscience and Remote Sensing Symposium (IGARSS), Milan, Italy, 13–18 July 2015. [[CrossRef](#)]
46. O'Leary, P.; Zsombor-Murray, P. Direct and specific least-square fitting of hyperbol[ae ligature] and ellipses. *J. Elec. Imaging* **2004**, *13*, 492–503.
47. Shihab, S.; Al-Nuaimy, W. Radius Estimation for Cylindrical Objects Detected by Ground Penetrating Radar. *Subsurf. Sens. Technol. Appl.* **2005**, *6*, 151–166. [[CrossRef](#)]
48. Zhang, P.; Guo, X.; Muhammat, N.; Wang, X. Research on probing and predicting the diameter of an underground pipeline by GPR during an operation period. *Tunn. Undergr. Space Technol.* **2016**, *58*, 99–108. [[CrossRef](#)]
49. Akritas, M.G.; Roussas, G.G. GPR characterization of buried tanks and pipes. *Geophysics* **1997**, *62*, 797–806.
50. Fu, X. The Characteristics and Application Points of Digital Storage Oscilloscope. *Off. Informatiz.* **2011**, *12*, 30–31.
51. Kim, J.O.; Hwang, K.-K.; Lee, J.-G.; Jeong, H.-G. Cylindrical transducers to generate and detect axisymmetric waves in a pipe. *J. Acoust. Soc. Am.* **2004**, *115*, 2575. [[CrossRef](#)]
52. Leighton, T.G.; Ramble, D.G.; Phelps, A.D.; Morfey, C.L.; Harris, P.P. Acoustic Detection of Gas Bubbles in a Pipe. *Acta Acust. United Acust.* **1998**, *84*, 801–814.
53. Mashford, J.; Rahilly, M.; Davis, P. An Approach Using Mathematical Morphology and Support Vector Machines to Detect Features in Pipe Images. In Proceedings of the 2008 Digital Image Computing: Techniques and Applications, Canberra, ACT, Australia, 1–3 December 2008; 2008; pp. 84–89.
54. Owowo, J.; Oyadiji, S.O. Finite element analysis and experimental measurement of acoustic wave propagation for leakage detection in an air-filled pipe. *Int. J. Struct. Integr.* **2017**, *8*, 452–467. [[CrossRef](#)]



© 2020 by the authors. Licensee MDPI, Basel, Switzerland. This article is an open access article distributed under the terms and conditions of the Creative Commons Attribution (CC BY) license (<http://creativecommons.org/licenses/by/4.0/>).